

## Synchronization in light-controlled oscillators

G.M. Ramírez Ávila<sup>a,b,\*,1</sup>, J.L. Guisset<sup>a</sup>, J.L. Deneubourg<sup>a</sup>

<sup>a</sup> Center for Nonlinear Phenomena and Complex Systems, Université Libre de Bruxelles,  
Campus Plaine CP231, 1050 Brussels, Belgium

<sup>b</sup> Instituto de Investigaciones Físicas, Universidad Mayor de San Andrés, Casilla 8635 La Paz, Bolivia

Received 2 July 2002; received in revised form 23 April 2003; accepted 24 April 2003

Communicated by Y. Kuramoto

### Abstract

We have built light-controlled oscillators (LCOs) that mimic gregarious fireflies in the sense that their interactions are episodic and almost pulse-like. The ability of the LCOs to synchronize their light emission constitutes a good experimental setup to validate different models of populations of integrate-and-fire oscillators and to analyze the role of the interactions and the spatial distribution of the LCOs. Experimental measurements on two and three interacting LCOs enable us to find synchronization ranges despite intrinsic differences among the oscillators. We develop a mathematical model that we have used to solve analytically the simplified case of two identical oscillators in which we have found synchronous and anti-synchronous states. We have constructed the phase response curve for an LCO. Finally, we solved the model numerically finding that it reproduces our different experimental results with two LCOs (master–slave interaction and mutual interaction) and three interacting LCOs in a linear configuration.

© 2003 Elsevier Science B.V. All rights reserved.

PACS: 05.45.Xt; 05.65.+b; 85.60.–q; 85.60.Dw; 89.75.–k

Keywords: Synchronization; Coupled oscillators; Collective behavior; Optoelectronic devices

### 1. Introduction

The phenomenon of synchronization has been studied in systems of very different nature varying from electronic devices to chemical, biological and ecological systems [1–12]. It may be understood as an adjustment of rhythms of self-sustained oscillators [13] that involves the development of a uniform rhythm in spite of intrinsic differences in individual rhythms and often extremely weak mutual connections. In the simplest case, when a synchronous process is achieved, the objects involved in this phenomenon start moving with the same frequencies in the presence of even very weak interactions. In such cases, definite phase relations between oscillations are maintained [14].

Examples of temporal synchronization and rhythmicity of activities abound in group-living organisms. Different classifications have been suggested. In the case where there is no leader (acting as an external pacemaker) in the

\* Corresponding author. Tel.: +3226505529; fax: +3226505767.

E-mail address: [gramirez@ulb.ac.be](mailto:gramirez@ulb.ac.be) (G.M. Ramírez Ávila).

<sup>1</sup> Partially supported by Belgian Technical Cooperation.

group, we distinguish two categories of rhythmicity. The first involves activities for which the individuals show no intrinsic rhythmicity but are rhythmic as a group, for example *Leptothorax* ants, whose colonies show synchronous rhythmic bursts of activity approximately every 20 min [15]. The second category involves activities in which each individual is rhythmic and the activity pattern becomes synchronized across the group. This category includes the synchronized choruses of crickets and cicadas, bee respiration, the synchronization of human female menstrual cycles and the synchronization of flashing among fireflies [16]. Thousands of fireflies gathered in certain swarm trees begin flashing soon after sunset, and synchrony builds up slowly through the night [17–20]. Each firefly acts as an intrinsic oscillator flashing at its own characteristic rhythm and is coupled to its neighbors through light perceived from other flashing fireflies in the sense that the sight of a neighbor's flash shifts the individual's rhythm. Synchronization is not imposed by any influence outside the system, such as a leader or external physical cue. Instead synchronization comes from within, based upon local and simple interactions between fireflies: a firefly's light emission shifts the timing of its neighbor's. The ability of a local group of synchronized individuals to capture additional oscillators is a form of positive feedback. Recently, it has been reported that synchrony occurs in the North American *Photuris frontalis*. These new results suggest that synchrony is common and pervasive rather than rare and sporadic [21].

The present work has been motivated by analogy with the phenomenon of synchronization that occurs in biological systems, in particular in groups of fireflies. The problem of synchronization among a population of oscillators has received considerable attention (see e.g. [22]), in part because of its intrinsic mathematical interest and in part because of the importance and ubiquity of such processes in biology [23–25]. Some of the research [25] has been inspired by a subject of considerable medical importance, the origin of synchronicity in the heart's natural pacemaker, a cluster of about 10 000 cells called the sino-atrial node [26–28]. Mirollo and Strogatz [25] have mathematically analyzed a population of oscillators interacting by means of a mechanism similar to that found in *Photinus pyralis*. Their model, however, makes some simplifying assumptions in the interest of mathematical tractability. They assume that all the oscillators in the population are identical, that the oscillator is sensitive to incoming light impulses throughout its charging cycle, jumping back instantly to zero when it fires, and that the increase in excitation is concave downward as in the electrical analog, rather than linear as assumed by Buck and Buck [17] and Buck et al. [29]. Under these assumptions, a population will become synchronized under almost all initial conditions. The system synchronizes rather slowly at first, but then synchronization builds up more rapidly [25].

Other work, e.g. [24] has been devoted to the analysis of pulse-coupled oscillators, following the model introduced by Mirollo and Strogatz with some variations such as the inclusion of inhibitory coupling. Although the analysis of a population of identical oscillators makes the problem more tractable mathematically, we would really like to know the properties of a system of realistic firefly oscillators, whose intrinsic flash frequencies are similar, but not identical. This more complicated situation has been discussed frequently (see e.g. [4,30]). The main conclusion is that, as the difference in the frequencies of the individual oscillators falls below a critical threshold, a portion of the system suddenly synchronizes. The combined signal of this synchronization cluster stands out above the background noise of random flashes and “captures” additional oscillators, further amplifying the collective signal. This infectious positive feedback results in an epidemic of synchrony.

Our main concern here is the synchronization between oscillators that in most cases are quantitatively different. This problem is very important in biological systems in which the oscillators in a group (e.g. fireflies of the same species, neighboring neurons) have intrinsic non-identical frequencies. Many examples of synchrony and phase locking of coupled oscillators have been documented in the literature but very few deal with the case of realistic pulse coupling systems. In this paper, we study the phenomenon of synchronization in a real physical system composed of LCOs coupled by light pulses. In Section 2, we present our oscillator, which is based on the construction proposed by Garver and Moss [31]. In Section 3, we set up a model that describes the behavior of our oscillator in isolation as well as the situation in which the devices interact; we also construct the phase response curve (PRC) for an LCO

in order to characterize it. In Section 4, we analytically solve a reduced system of two identical oscillators. Finally, in Section 5 we compare the experimental and numerical results.

## 2. The oscillator

The LCO we use in our phase locking experiments consists of an LM555 chip wired (Fig. 1(a)) to function in astable oscillating mode [32]. As such the LCO behaves as a relaxation oscillator whose period is related to the charge and discharge of the two external RC circuits with resistances  $R_\lambda + R_\gamma$  and  $R_\gamma$  (Fig. 1(a)). This astable mode is simple to describe. The LM555 combines three functions. Firstly, it measures the voltage across the capacitor  $C$ . Secondly, it may or may not establish a short-circuit across the RC components. Finally, it produces an on–off signal at its output. When the short-circuit is established, the capacitor discharges through  $R_\gamma$ . Without the short-circuit, the capacitor charges through  $R_\lambda + R_\gamma$ . It switches from the discharging state to the charging state when it detects

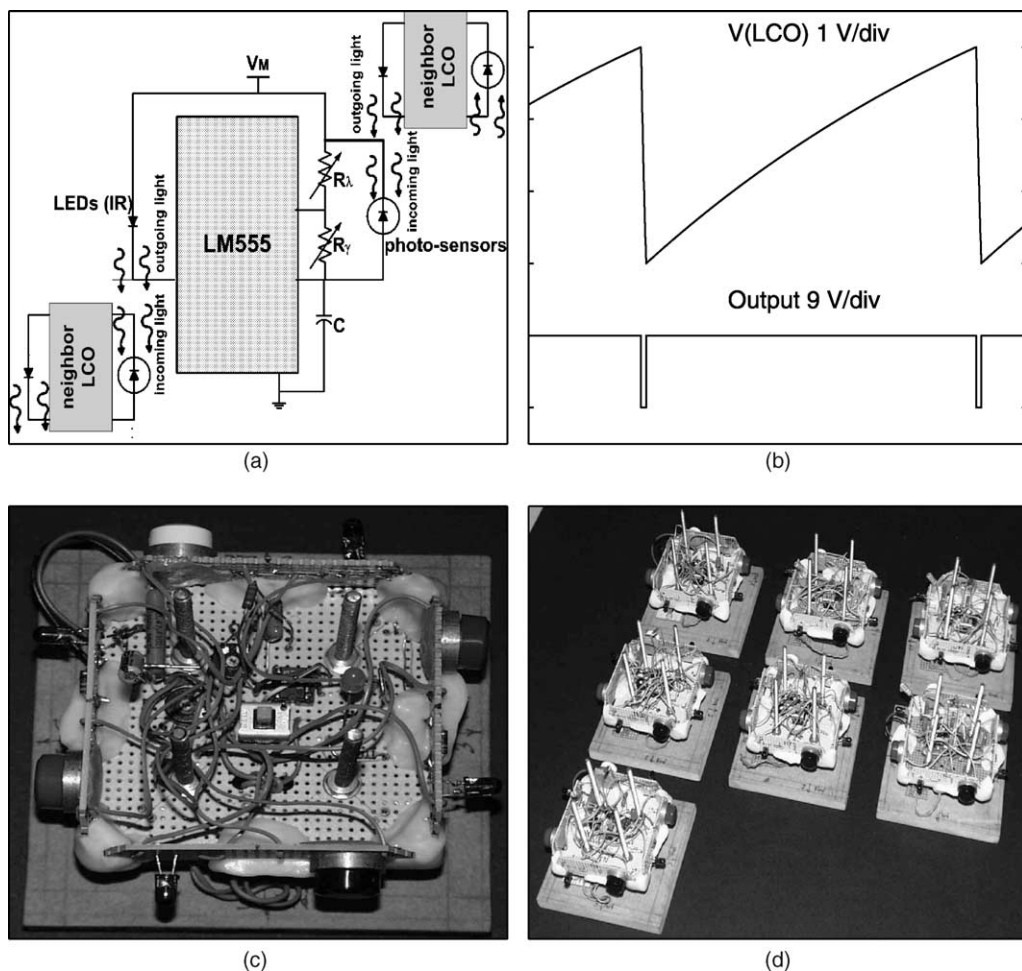


Fig. 1. (a) Block diagram of the LCO and schematic view of the coupling between LCOs. (b) Signal at the terminals of the timing capacitor. The values used are:  $R_\lambda = 100 \text{ k}\Omega$ ,  $R_\gamma = 1.6 \text{ k}\Omega$  and  $C = 0.47 \text{ }\mu\text{F}$ . The thresholds are  $V_M/3 = 3 \text{ V}$  and  $2V_M/3 = 6 \text{ V}$ . (c) View of a single LCO. (d) LCOs arranged for mutual interaction.

a third of the supply voltage ( $V_M/3$ ) and it returns to the discharging state, when it detects  $2V_M/3$ . The circuit triggers itself and the output waveform takes the form of a pulse signal with minimum and maximum values set at  $V_M/3$  and  $2V_M/3$ , respectively (Fig. 1(b)).  $R_\lambda$  and  $R_\gamma$  can be modified manually and are used to preset the two time intervals of the period. The period is the sum of two unequal time intervals: the longer interval, related to the time constant  $1/\lambda = (R_\lambda + R_\gamma)C$ , corresponds to the charging time of the capacitor; the shorter interval corresponds to the discharge of the same capacitor and is related to  $1/\gamma = R_\gamma C$ . The charging and the discharging stages are described by the equations:

$$\frac{dV}{dt} = \lambda(V_M - V) \quad (\text{charge}), \quad \frac{dV}{dt} = -\gamma V \quad (\text{discharge}). \quad (1)$$

Photo-sensors wired in parallel with  $R_\lambda$  and  $R_\gamma$  [31] modify both time constants when illuminated. A pulse of IR light is produced at each period, lasting for the shorter discharging state. The IR light beam is directed to the photo-sensors of the neighboring LCOs (Fig. 1(a)), establishing optical coupling. Depending on the phase difference between interacting LCOs, an IR flash causes a neighbor to shorten the longer part of its period (phase advance) and to lengthen the shorter part (phase delay).

To achieve global synchrony, the time constants of each of the LCOs had to be adjusted in the dark so that the longer and shorter parts of their periods would be fairly similar. We refer to these periods as “dark periods” (natural periods), i.e. where there is no interaction between neighboring LCOs. Darkness is obtained by masking the photo-sensors mechanically. Each LCO is equipped with removable masks, making it possible to preset their dark period in a reproducible way; this allows us to determine synchronization ranges and the corresponding phase dependence with adequate accuracy [33,34]. Experimentally, we can study several LCO’s configurations: in a line, in a square, in a cross or in a lattice (Fig. 1(d)), but in this paper we have only performed phase difference measures for two and three LCOs in a line, in which we had to pay attention to the distance ( $d$ ) between the LCOs since it determines the strength of the optical coupling.

Using the physics related to the explanation of our oscillator (charge and discharge of the external RC circuits and the optical coupling), we can formulate a simple model that describes the functioning of individual and coupled LCOs.

### 3. Model

The mathematical model is linked to the dual state structure of the LCO’s period. We describe the state of the  $i$ th LCO state by the binary variable  $\epsilon_i(t)$ :

$$\epsilon_i(t) = 1 : \text{extinguished LCO (charging stage)}, \quad \epsilon_i(t) = 0 : \text{fired LCO (discharging stage)}.$$

A “blind” LCO, isolated from any external light likely to modify its period, may be described during its charging and its discharging processes by standard equations for the capacitor that we introduced in Section 2:

$$\begin{aligned} \frac{dV_i(t)}{dt} &= \lambda_i(V_{Mi} - V_i(t))\epsilon_i(t), & \frac{V_{Mi}}{3} \leq V_i(t) \leq \frac{2V_{Mi}}{3}, & \epsilon_i(t) = 1, \\ \frac{dV_i(t)}{dt} &= -\gamma_i V_i(t)(1 - \epsilon_i(t)), & \frac{2V_{Mi}}{3} > V_i(t) > \frac{V_{Mi}}{3}, & \epsilon_i(t) = 0. \end{aligned} \quad (2)$$

The transition between the two states constituting the LCO’s period is described by the following relation:

$$\text{If } V_i(t) = \frac{V_{Mi}}{3} \text{ and } \epsilon_i(t) = 0, \text{ then } \epsilon_i(t_+) = 1, \quad \text{If } V_i(t) = \frac{2V_{Mi}}{3} \text{ and } \epsilon_i(t) = 1, \text{ then } \epsilon_i(t_+) = 0. \quad (3)$$

Solving the charge and discharge equations in (2) and using (3), we can find the natural period  $T$  of an LCO:

$$T = t_\lambda + t_\gamma = (R_\lambda + 2R_\gamma)C \ln 2,$$

where

$$t_\lambda = (R_\lambda + R_\gamma)C \ln 2 \quad (\text{integrating stage of the period})$$

and

$$t_\gamma = R_\gamma C \ln 2 \quad (\text{firing stage of the period})$$

are the durations of the charging and discharging processes, respectively.

When the LCO's optical sensors are not blinded, the period of an LCO may be modified by the surrounding light and by the IR light beams of neighboring LCOs. Let  $\beta_{ij}$  be the change in  $dV_i/dt$  of LCO $_i$  due to the IR light produced by LCO $_j$ . Let  $\delta_{ij}$  indicate whether or not there is an interaction between LCO $_i$  and LCO $_j$ :  $\delta_{ij} = 1$  when there is an interaction,  $\delta_{ij} = 0$  when there is no interaction, and  $\delta_{ii} = 0$  always, to denote no self-interaction. We can then write:

$$\frac{dV_i(t)}{dt} = \lambda_i(V_{Mi} - V_i(t))\epsilon_i(t) - \gamma_i V_i(t)[1 - \epsilon_i(t)] + \sum_{j=1}^N \beta_{ij}\delta_{ij}[1 - \epsilon_j(t)], \quad i, j = 1, \dots, N. \quad (4)$$

Note that the interaction term is active only when at least one of the other LCOs is discharging. In this model and for our experiments, we will consider symmetric interactions, such that  $\beta_{ij} = \beta_{ji}$ .

### 3.1. Phase response curves

A PRC is a plot of the magnitude of the phase shift due to a pulse versus the time at which the pulse was applied. Usually, PRCs are used in research dealing with circadian rhythms [35–37] but also they are used to a great extent in other biological oscillators [38–40]. The goal of this subsection is to characterize our LCO with this classical tool that enables us to examine how a perturbation shifts the phase of the oscillator. The phase shift is defined as [39,41]:

$$\Delta(\phi) = \frac{T - T^*(\phi)}{T}, \quad (5)$$

where  $T$  represents the natural period and  $T^*(\phi)$  the new period of the oscillator being perturbed. In order to show clearly how the PRC can be obtained for an LCO, we define an arbitrary zero phase for the LCO signal; for convenience, we take it to be when the signal is just in the middle of the thresholds in the discharging stage, so it has the voltage value  $V_M/2$  (usually, the zero phase is taken just after the voltage peak as in [34]). This choice enables us to take into account the regions where there are transitions from one stage to the other; these regions are particularly interesting because during a transition there can be both effects: advance or delay in the phase. The last was shown experimentally in [33,34].

We begin by defining some parameters that we will use to determine the period of the signal (Fig. 2(a)). We remark that in order to show the transition regions clearly, Fig. 2 has been obtained using a value of 16 k $\Omega$  for  $R_\gamma$ , which constitutes 10 times the usual experimental value. A perturbation applied to the oscillator will generate either an advance or a delay in the phase and it is a function of the magnitude and the timing of the perturbation [41]. In (5),  $\Delta(\phi)$  is positive (negative) if the perturbation acts to advance (retard) the time of the next event [41]. For our LCOs, we can compute the PRCs exactly. Considering the equations of the model, we can integrate the equation for

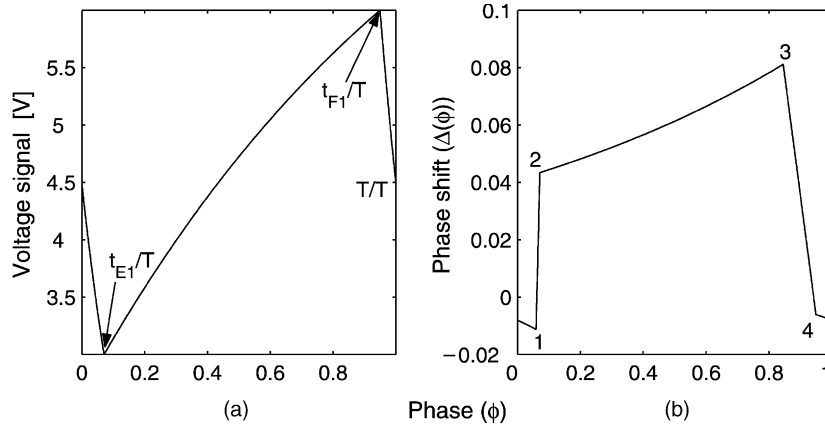


Fig. 2. (a) Parameter definition to determine the PRC.  $t_{E1}$  and  $t_{F1}$  represent the LCO's extinction time and the LCO's firing time, respectively (without perturbation). (b) PRC obtained from analytical solution of the LCO's differential equations. Points 1, 2, 3, and 4 are related to  $t_{E1}^{*(2)}$ ,  $t_{E1}$ ,  $t_{F1}^{*(4)}$ , and  $t_{F1}$ , respectively (see text).

an LCO when a perturbation  $\beta$  (interaction strength) acts during a short time interval  $\tau = t_f - t_0$ ,  $t_0$  and  $t_f$ , being the times when the stimulus begins and finishes, respectively. The solutions are

$$V(t) = V(t_0) e^{-\lambda(t-t_0)} + \left( V_M + \frac{\beta}{\lambda} \right) (1 - e^{-\lambda_i(t-t_0)}), \tag{6}$$

when the perturbation acts on the charging stage, and

$$V(t) = V(t_0) e^{-\gamma(t-t_0)} + \frac{\beta}{\gamma} (1 - e^{-\gamma_i(t-t_0)}), \tag{7}$$

when it acts on the discharging stage. Firstly, we define some useful parameters for our description. Let  $t_{E1}$ ,  $t_{F1}$  be the times when the LCO achieves its lower ( $V_M/3$ ) and its upper threshold ( $2V_M/3$ ), respectively, when there is no perturbation. Similarly,  $t_{E1}^*$ ,  $t_{F1}^*$  are the times when a stimulus is acting on the LCO. The constants  $t_\lambda$  (duration of the charging stage) and  $t_\gamma = t_{\gamma_1} + t_{\gamma_2} = (\ln(3/2)/\gamma) + (\ln(4/3)/\gamma)$  (duration of the whole discharging stage), where  $t_{\gamma_1}$  and  $t_{\gamma_2}$  are the times taken to go from  $V_M/2$  to  $V_M/3$ , and from  $2V_M/3$  to  $V_M/2$ , respectively. Second, we can identify defined regions that appear due to the discontinuity of the model. We shall find  $T^*$  related to each region.

Region 1: If  $0 \leq t_0 < t_{E1}^{*(2)} - \tau$ , then

$$T^*(\phi) = t_{E1}^{*(1)} + t_\lambda + t_{\gamma_2}, \tag{8}$$

where

$$t_{E1}^{*(1)} = \frac{1}{\gamma} \ln \left[ \frac{3}{2} + \frac{3\beta}{V_M\gamma} (e^{\gamma t_f} - e^{\gamma t_0}) \right].$$

Region 2: If  $t_{E1}^{*(2)} - \tau \leq t_0 < t_{E1}$ , then

$$T^*(\phi) = t_{E1}^{*(2)} + t_{\gamma_2}, \tag{9}$$

where

$$t_{E1}^{*(2)} = t_{\gamma_1} + \frac{1}{\gamma} \ln \left( \frac{V_M\gamma - 2\beta e^{\gamma t_0}}{V_M\gamma - 3\beta} \right)$$

and

$$t_{F1}^{*(2)} = \frac{1}{\lambda} \ln \left[ 2e^{\lambda t_{E1}^{*(2)}} + \frac{3\beta}{V_M \lambda} (e^{\lambda t_{E1}^{*(2)}} - e^{\lambda t_f}) \right].$$

*Region 3:* If  $t_{E1} \leq t_0 < t_{F1}^{*(4)} - \tau$ , then

$$T^*(\phi) = t_{F1}^{*(3)} + t_{\gamma 2}, \quad (10)$$

where

$$t_{F1}^{*(3)} = \frac{1}{\lambda} \ln \left[ 2e^{\lambda t_{E1}} + \frac{3\beta}{V_M \lambda} (e^{\lambda t_0} - e^{\lambda t_f}) \right].$$

*Region 4:* If  $t_{F1}^{*(4)} - \tau \leq t_0 < t_{F1}$ , then

$$T^*(\phi) = t_{\gamma} + \frac{1}{\gamma} \ln \left[ \frac{2}{3} e^{\gamma t_{F1}^{*(4)}} - \frac{\beta}{V_M \gamma} (e^{\gamma t_{F1}^{*(4)}} - e^{\gamma t_f}) \right], \quad (11)$$

where

$$t_{F1}^{*(4)} = \frac{1}{\lambda} \ln \left( \frac{2V_M \lambda e^{\lambda t_{E1}} + 3\beta e^{\lambda t_f}}{V_M \lambda + 3\beta} \right).$$

*Region 5:* If  $t_{F1} \leq t_0 \leq T$ , then

$$T^*(\phi) = t_{\gamma} + \frac{1}{\gamma} \ln \left[ \frac{2}{3} e^{\gamma t_{F1}} - \frac{\beta}{V_M \gamma} (e^{\gamma t_0} - e^{\gamma t_f}) \right]. \quad (12)$$

To construct the PRC, we can join Eqs. (8)–(12) in the form of a piecewise equation or integrate numerically the differential equations of the model. Fig. 2(b) shows a typical PRC obtained for an LCO; this is slightly different to a typical integrate-and-fire PRC [41] because LCO's phase can both advances and retards. As could expect, the shape of this curve is not smooth due to the discontinuities of the model. We observe four points where the shape of the curve changes dramatically.

Fig. 3 shows how the phase advances or is delayed due to a perturbation.

In Fig. 4, we show some PRCs for different strengths and different durations of the stimulus. We can observe that as could be expected, the PRCs are modified by both the strength and the duration of the stimulus. Finally, it could be possible to construct the phase transition maps in order to use these to couple the PRCs and analyze the synchronization by these means. However, in this paper we only work with analytical solutions for two identical LCOs (see Section 4) and numerical integration that shows a good agreement between numerical and experimental results (see Section 5).

#### 4. Two identical oscillators

Here we analyze Eq. (4) for two identical coupled oscillators ( $\lambda_1 = \lambda_2 = \lambda$ ,  $\gamma_1 = \gamma_2 = \gamma$ ,  $V_{M1} = V_{M2} = V_M$ ). We neglect the modification in the discharging process due to the interaction, i.e. the time  $\Delta$  of the discharging process (duration of an interaction) remains constant and equal to the duration of the light pulse of an isolated LCO ( $\Delta = t_{\gamma} = \ln 2/\gamma$ ). The voltage across the timing capacitor is computed for each of the interacting LCOs;

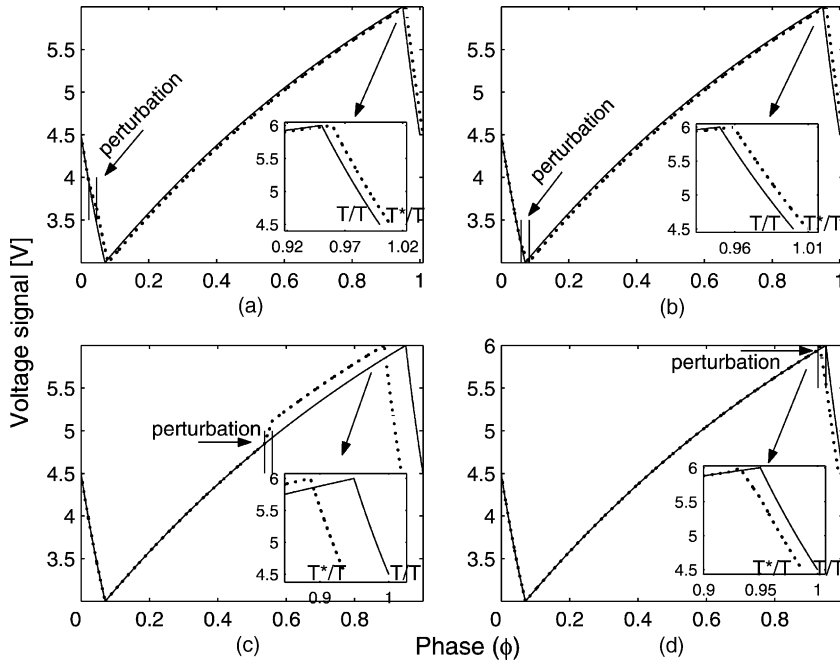


Fig. 3. Effects of a stimulus in an LCO. In each graph, the perturbation is represented by vertical lines and the region where the signal reaches the entire cycle is magnified showing whether the phase is advanced or delayed. (a) Stimulus in region 1 and its effect on phase is equivalent to one in region 5, it delays the LCO’s phase. (b) Region 2 (transition discharging–charging stage); there can exist advance or delay in the LCO’s phase. (c) Region 3, only advance of the LCO’s phase. (d) Region 4, similar behavior as in (b), advance or delay of the LCO’s phase.

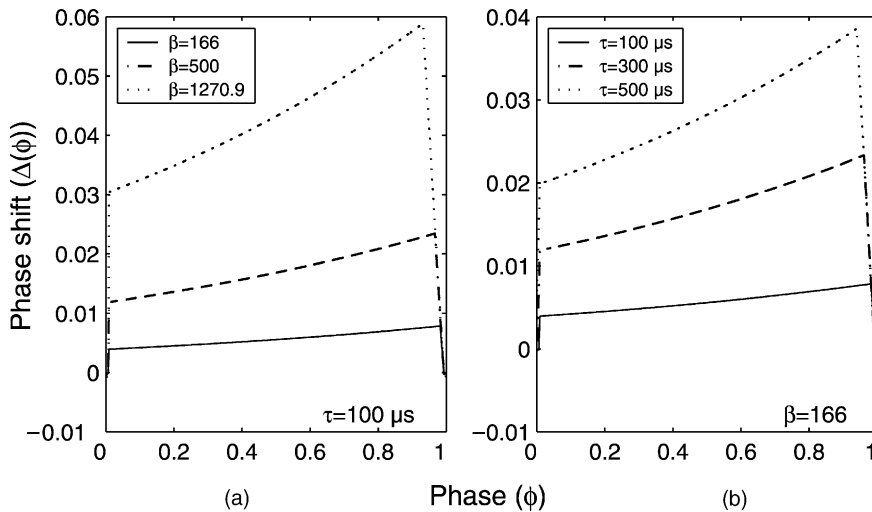


Fig. 4. PRCs for an LCO when the parameters are:  $R_\lambda = 100 \text{ k}\Omega$ ,  $R_\gamma = 1.6 \text{ k}\Omega$  and  $C = 0.47 \text{ }\mu\text{F}$ . (a) Different strengths when the stimulus duration is  $\tau = 100 \text{ }\mu\text{s}$ . (b) Different perturbation durations when the strength is  $\beta = 166$ .

the solution when LCO<sub>j</sub> is acting on LCO<sub>i</sub>, the latter being in its charging stage is obtained rewriting (6) with t<sub>0</sub> replaced by t<sub>Fj</sub>:

$$V_i(t) = V_i(t_{Fj}) e^{-\lambda(t-t_{Fj})} + \left( V_M + \frac{\beta}{\lambda} \right) (1 - e^{-\lambda(t-t_{Fj})}), \tag{13}$$

where t<sub>Fj</sub> is the flashing time of LCO<sub>j</sub>, i.e. when the interaction with LCO<sub>i</sub> begins, and V<sub>i</sub>(t<sub>Fj</sub>) is the voltage of LCO<sub>i</sub> at time t<sub>Fj</sub>.

Assuming that the interaction time is short and the interaction between oscillators is sufficient (|β| > |λ|) to dominate the solution (13), we approximate the effect of the interaction over the charging cycle by dV<sub>i</sub>(t)/dt = β, obtaining V<sub>i</sub>(t) = V<sub>i</sub>(t<sub>Fj</sub>) + βt. This enables us to work with simple expressions that are not too far from the results obtained from the numerical solution. These simplifications are used throughout this section.

Firstly, we describe a situation where the short impulses overlap (Fig. 5). The phase difference Δφ between the oscillators is proportional to the time difference between their flashing times t<sub>F1</sub>, t<sub>F2</sub>, or between their extinction times t<sub>E1</sub>, t<sub>E2</sub>. Taking this into account, the phase differences during the first and second firings are given by

$$\frac{T}{2\pi} \Delta\phi_{12} = t_{F1} - t_{F2} = \frac{V_M}{3\beta} \frac{V_{02} - V_{01}}{V_M - V_{02}}, \quad \frac{T}{2\pi} \Delta\phi'_{12} = \frac{V_M}{3\beta} \frac{V_{02} - V_{01}}{2V_M - 3V_{02} + V_{01}}.$$

Further calculation yields:

$$\frac{T}{2\pi} \Delta\phi_{12}^{(n)} = \frac{V_M}{3\beta} \left[ \frac{V_{02} - V_{01}}{2^{n-1}V_M - (2^n - 1)V_{02} + (2^{n-1} - 1)V_{01}} \right] < \Delta, \tag{14}$$

where V<sub>01</sub> and V<sub>02</sub> are the initial conditions for LCOs 1 and 2, respectively. As n tends to infinity, the phase difference tends toward zero, which indicates perfect overlapping of the signals with phase locking between the LCOs. Setting

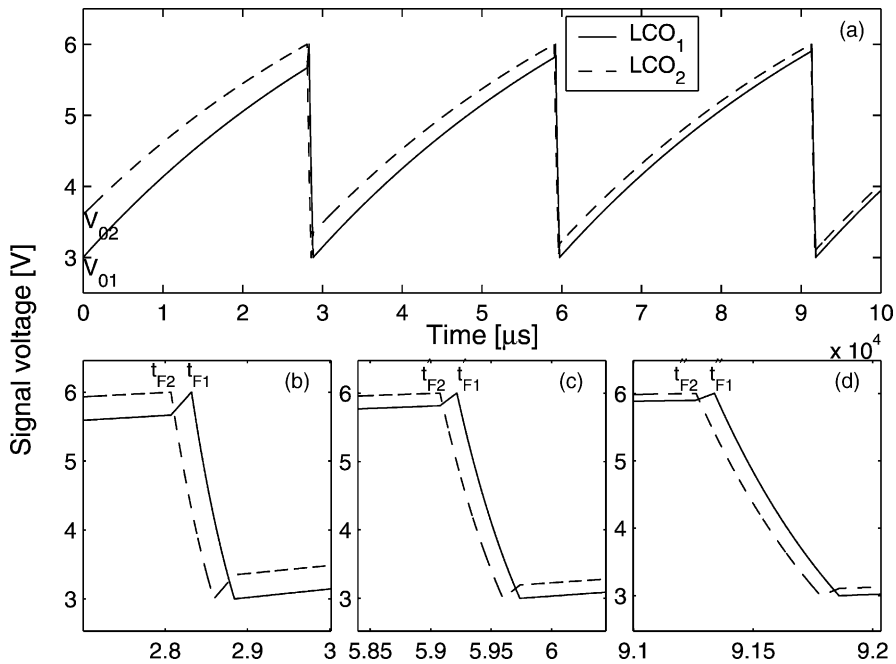


Fig. 5. Overlapped signals show us the tendency toward zero phase difference. (a) Evolution of the LCO's signals when the short impulses overlap. The shape of the signals are magnified in (b), (c) and (d) for the first, second and third firing regions, respectively.

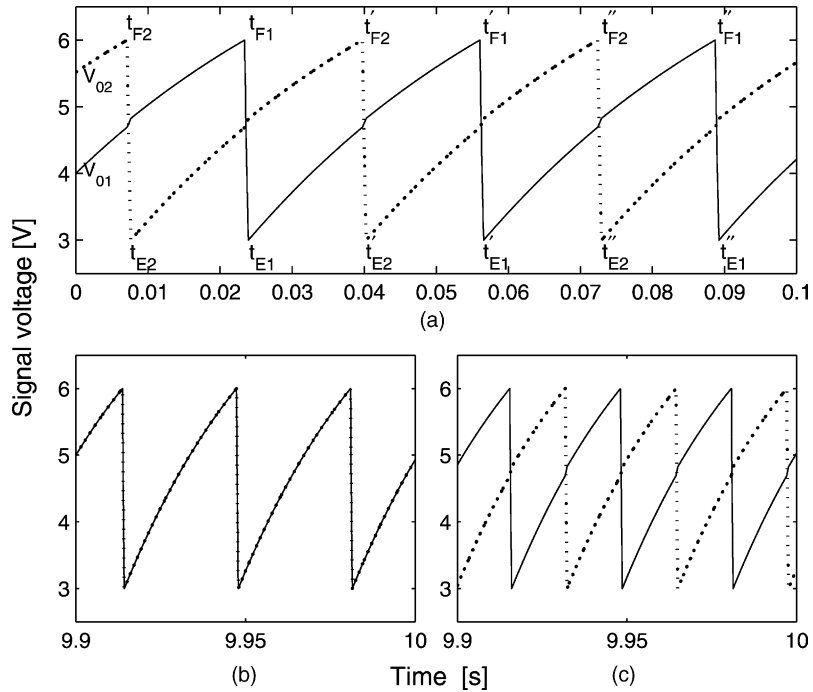


Fig. 6. (a) Non-overlapping signals for two identical oscillators.  $t_F$  and  $t_E$  indicate the time of flashing and extinction, respectively. (b) Subsequent synchronous state ( $\Delta\phi_{12}^{(n)} \rightarrow 0$ ) when the initial conditions were  $V_{01} = 4.0$  V and  $V_{02} = 5.5178$  V. (c) Anti-synchronous stationary state ( $\Delta\phi_{12} = \Delta\phi_{12}^{(n)} = \text{constant}$ ) when the initial conditions were  $V_{01} = 4.0$  V and  $V_{02} = 5.5181$  V. The parameter values are the same that we used in Fig. 4.

$\beta\Delta = x$ , we can find a condition for  $V_{02}$  when the signals overlap in the short part of the period:

$$V_{02} < \frac{V_M(3x + V_{01})}{V_M + 3x}. \tag{15}$$

On the other hand, if the signals do not overlap (Fig. 6(a)), the inequality (15) reverses and the phase difference may evolve as  $\Delta\phi_{12} \begin{matrix} \geq \\ \leq \end{matrix} \Delta\phi'_{12}$ . Taking into account the approximation mentioned earlier, we can write the expressions for the LCO's signals for each region explicitly. For instance, when  $V_{02} > V_{01}$ , we obtain the solution for the first charging process and the discharging process of LCO<sub>2</sub>:

$$V_2 = V_{02} e^{-\lambda t} + V_M(1 - e^{-\lambda t}), \quad V_2 = \frac{2}{3} V_M e^{-\gamma(t-t_{F2})} \tag{16}$$

and for the first charging process of LCO<sub>1</sub>:

$$V_1 = [V_M(1 - e^{-\lambda t_{F2}}) + V_{01} e^{-\lambda t_{F2}} + \beta(t_{E2} - t_{F2})] e^{-\lambda(t-t_{E2})} + V_M(1 - e^{-\lambda(t-t_{E2})}). \tag{17}$$

Using the expressions above, we find that the equations for the flashing and extinction times are

$$t_{F2} = -\frac{1}{\lambda} \ln \left[ \frac{V_M}{3(V_M - V_{02})} \right], \quad t_{E2} = \frac{\ln 2}{\gamma} + t_{F2},$$

$$t_{F1} = -\frac{1}{\lambda} \ln \left[ \frac{V_M/3}{(V_M - V_{01}) e^{-\lambda t_{F2}} - \beta(t_{E2} - t_{F2})} \right] + t_{E2}, \quad t_{E1} = \frac{\ln 2}{\gamma} + t_{F1}. \tag{18}$$

The general equations ( $n = 2, \dots$ ) are obtained by recurrence:

$$\begin{aligned} t_{F2}^{(n)} &= \frac{1}{\lambda} \ln \left[ 2 e^{-\lambda(t_{F1}^{(n-1)} - t_{E2}^{(n-1)})} - \frac{3x}{V_M} \right] + t_{E1}^{(n-1)}, & t_{E2}^{(n)} &= \frac{\ln 2}{\gamma} + t_{F2}^{(n)}, \\ t_{F1}^{(n)} &= \frac{1}{\lambda} \ln \left[ 2 e^{-\lambda(t_{F2}^{(n)} - t_{E1}^{(n)})} - \frac{3x}{V_M} \right] + t_{E2}^{(n)}, & t_{E1}^{(n)} &= \frac{\ln 2}{\gamma} + t_{F1}^{(n)}. \end{aligned} \quad (19)$$

With these expressions, and using the fact that phase and time differences are related by  $\Delta\phi_{ij} = 2\pi(t_{Fi} - t_{Fj})/T$ , we can find and compare the successive phase differences  $\Delta\phi_{12}$  and  $\Delta\phi'_{12}$ , and since  $\Delta\phi_{12} \begin{smallmatrix} \geq \\ \leq \end{smallmatrix} \Delta\phi'_{12}$  we obtain:

$$(V_{02} - y^+)(V_{02} - y^-) \begin{smallmatrix} \geq \\ \leq \end{smallmatrix} 0, \quad (20)$$

where

$$y^\pm = V_M + \frac{3x}{4V_M}(V_M - V_{01}) \left[ 1 \pm \sqrt{1 + 2 \left( \frac{2V_M}{3x} \right)^2} \right]. \quad (21)$$

The only acceptable solution, imposed by the experimental conditions is  $y^-$ ;  $y^+$ , being greater than  $V_M$ , is discarded.  $y^-$  corresponds to an unstable stationary anti-synchronous regime without phase locking, with  $\Delta\phi_{12} = \Delta\phi'_{12}$ . Indeed, if  $V_{02} = y^-$ ,  $(V_{02} - y^+)(V_{02} - y^-) = 0$  and the LCOs do not change their phase differences, and if  $V_{02} \neq y^-$ , the phase difference tends to decrease or increase until the signals overlap corresponding to phase locking. Summarizing:

- if  $V_{02} < y^-$ ,  $(V_{02} - y^+)(V_{02} - y^-) > 0$ , the phase difference decreases,
- if  $V_{02} > y^-$ ,  $(V_{02} - y^+)(V_{02} - y^-) < 0$ , the phase difference increases.

The latter was found with the condition  $V_{02} > V_{01}$ . Nevertheless, analogous results can be obtained considering  $V_{01} > V_{02}$ :

$$(V_{02} - z^+)(V_{02} - z^-) \begin{smallmatrix} \geq \\ \leq \end{smallmatrix} 0, \quad (22)$$

where

$$z^\pm = V_M - \frac{3x}{2V_M}(V_M - V_{01}) \left[ 1 \pm \sqrt{1 + 2 \left( \frac{2V_M}{3x} \right)^2} \right], \quad (23)$$

$z^+$  being the only acceptable solution since  $z^- > V_M$  must be discarded.  $V_{02} = z^+$  corresponds to the anti-synchronous stationary state. Otherwise, as in the preceding case, the phase difference increases or decreases but it always tends to the overlapping situation with phase locking.

Now, if we label one of the oscillators as the “reference LCO” ( $\text{LCO}_{\text{ref}}$ ), the description of the other oscillator can be carried out in terms of  $\text{LCO}_{\text{ref}}$ . This enables us to write a general solution obtained under the condition that phase difference remains constant and the constraints imposed by our experimental conditions are applied:

$$V_0^\pm = \begin{cases} V_M - \frac{3x}{2V_M}(V_M - V_{0\text{ref}}) \left[ 1 + \sqrt{1 + 2 \left( \frac{2V_M}{3x} \right)^2} \right] & \text{if } V_0 < V_{0\text{ref}}, \\ V_M + \frac{3x}{4V_M}(V_M - V_{0\text{ref}}) \left[ 1 - \sqrt{1 + 2 \left( \frac{2V_M}{3x} \right)^2} \right] & \text{if } V_0 > V_{0\text{ref}}. \end{cases} \quad (24)$$

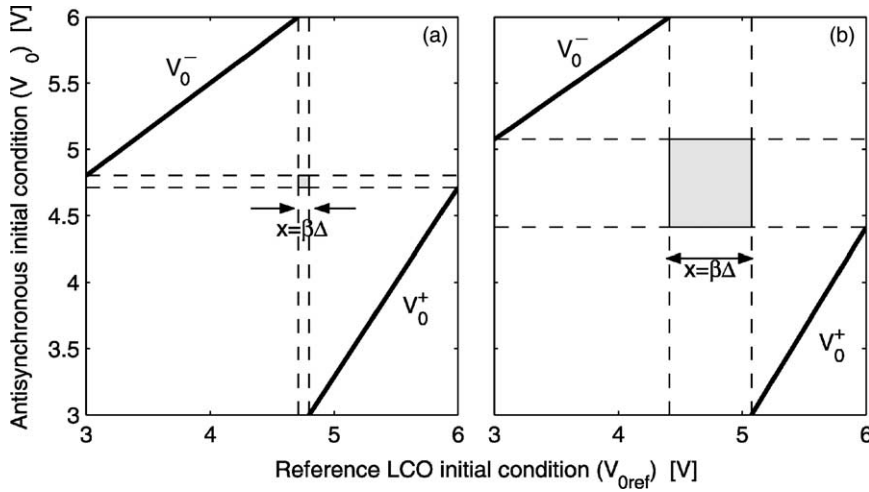


Fig. 7. Synchronization criterion for different interaction values: (a)  $\beta = 166.0$ , and (b)  $\beta = 1270.9$ . The parameter values used are the same as in Fig. 4.

Indeed, in (24) we had two solutions for each initial condition  $(V_0^+, V_0^-)$  since the fact that  $\Delta\phi_{12} = \Delta\phi'_{12}$  results in a quadratic equation but the only acceptable solutions according to the experimental parameters are  $V_0^+$ , related to  $z^+$  when  $V_0 < V_{0\text{ref}}$  and  $V_0^-$  related to  $y^-$  when  $V_0 > V_{0\text{ref}}$ . Actually, the region of interest is constrained to  $[V_M/3, 2V_M/3]$  on each axis. Thus for  $V_M = 9.0\text{ V}$  (voltage source value), the plot must be constrained to  $[3.0, 6.0]\text{ V}$  (Fig. 7). Thus, the anti-synchronous state can be obtained by starting the computation with LCOs' assigned appropriate initial conditions. We constructed two areas working with different strength values  $\beta$ . The intersections of the lines sketched from the extremal points delimit an area which increases with the strength  $\beta$ , indicating a region of synchronization (see Fig. 7). The area can be calculated by straightforwardly replacing the extremal values in Eq. (24). Taking  $V_0^- = 2V_M/3$  and  $V_0^+ = V_M/3$ , we obtain the abscissas:

$$V_{0\text{ref}}^- = V_M + \frac{4V_M^2}{9x(1 - \sqrt{1 + 2(2V_M/3x)^2})}, \quad V_{0\text{ref}}^+ = V_M - \frac{4V_M^2}{9x(1 + \sqrt{1 + 2(2V_M/3x)^2})}.$$

Then  $l = V_{0\text{ref}}^+ - V_{0\text{ref}}^- = x = \beta\Delta$  is the side length of the square area depicted in Fig. 7. If we take the initial conditions included in this area, we can affirm that there will not exist an anti-synchronization point and the system will always tend toward a phase locked state. We observe that the depicted area decreases when the strength of the coupling also decreases. In the limit as  $\beta \rightarrow 0$ , there will be only one intersection point, indicating that both oscillators should have the same initial conditions in order to have the same frequency, i.e. under these conditions there will exist a synchronization state achieved instantly (without phase locking).

Numerical integration confirms analytical results showing that there exists for  $\beta > 0$  initial conditions corresponding to an unstable anti-synchronous state. We can observe this in the top plots of Fig. 8, where we have represented the trajectories obtained by numerical integration for a situation in which the system remains in its anti-synchronous state. It is well known that the local stability of a state is determined by small perturbations [39,42]. If a state is reestablished, then it is stable as in the most cases of two identical coupled LCOs. If, on the other hand, a small perturbation induces a change in the dynamics (phase space) so that the original dynamics is not reestablished, then the state is unstable, as in the case of two identical coupled LCOs in anti-synchronization, where a perturbation has the consequence that the trajectory in the phase space changes with the tendency toward the limit cycle. The anti-synchronous state is unstable because a small perturbation takes the system out of its initial state

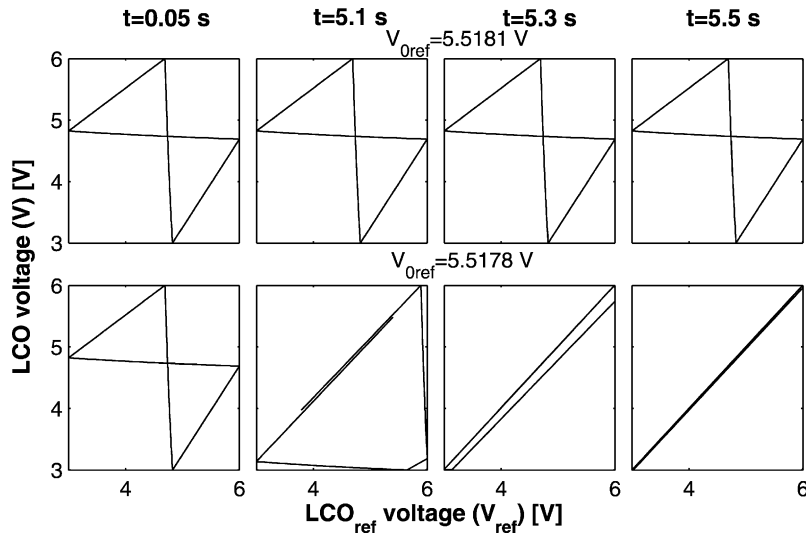


Fig. 8. Representation of the evolution of trajectories in the phase space for two identical coupled LCOs. Top: initial condition ( $V_0 = 4.0$  V,  $V_{0ref} = 5.5181$  V) related to an anti-synchronous state. Bottom: initial condition ( $V_0 = 4.0$  V,  $V_{0ref} = 5.5178$  V) viewed as a small perturbation of the anti-synchronous state. We can clearly note the tendency toward the limit cycle.

with consequent evolution towards the limit cycle shown in Fig. 8 (bottom). These results confirm our analysis using (20) and (22). In Fig. 9, we observe as well that if we are near the anti-synchronization point (initial conditions) there is a dramatic rise in the synchronization time, suggesting that this point is unstable because small perturbation allows the system to achieve in-phase synchronization. We also note from Fig. 9 that same strengths drive the system

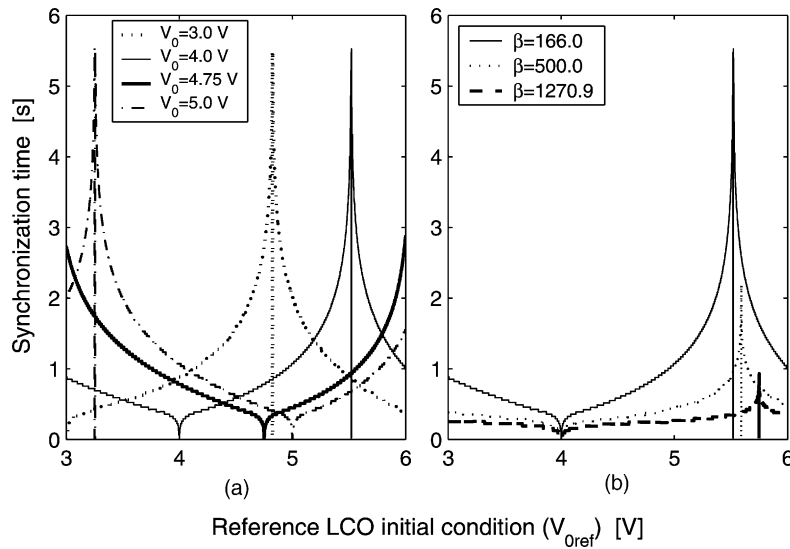


Fig. 9. Synchronization time as a function of the initial condition of the reference LCO. (a) Different initial conditions of one LCO using  $\beta = 166.0$ . We observe that for a particular initial condition, in this case  $V_0 = 4.75$  V, included in the area depicted in Fig. 7(a), the system never reaches the anti-synchronous state. (b) Different interaction strengths when  $V_0 = 4.0$  V. The parameter values are the same as in Fig. 4.

to synchronize with the same mean time. Finally, we can see that the synchronization time  $t_s$  decreases with an increase in the strength  $\beta$  as  $t_s \propto \beta^{-1}$ , and the graph of synchronization time as a function of the reference LCO initial condition confirms the criterion presented in Fig. 7. To conclude, we must point out that the analytical results obtained in this section are in close agreement with the numerical results obtained using (3) and (4), despite the simplifications introduced for this analysis.

The existence of in-phase and anti-phase synchronous states obtained from this simplified analysis coincides with the well-known results for two nearly identical clocks, in which both in-phase and anti-phase synchronization were reported [14], or the same results as stated in [23], where the coupled oscillators are viewed as identical components of a central pattern generator. The number of stable and unstable states and their phase differences may vary when the coupling and the dynamics of the oscillators are more complex.

Combination of these factors can clarify certain aspects (e.g. measurement of synchronization time, existence of unstable states) that are not easily solved by experiment.

## 5. Experimental measurements and comparison with the model

From an experimental point of view, synchrony between two or more oscillators is achieved if it is possible to observe stable phase differences between them. In practice, we perform phase measurements with 0.1% precision using Tektronix TDS 3012 oscilloscopes [33]. We measure the LCO phase changes caused by manual modifications of the period of one of the oscillators (reference LCO) (see Section 2), thereby determining the range in which phase locking is maintained, i.e. the synchronization range ( $\Delta T$ ). Several situations were studied: master–slave configuration, two interacting LCOs and three interacting LCOs in line. Despite the differences between them, synchronization is reached and it exhibits robustness under environmental perturbations or intrinsic statistical variations.

### 5.1. Measurements on a set of two LCOs

The simplest interaction is a one-way coupling that occurs when a master-LCO illuminates a slave-LCO. The one-way coupling may be implemented very simply by masking the master’s photo-sensors. In practice, we also used a pulse generator (PG) acting as the master oscillator [33] in which the period and the pulse width can be modified independently.

#### 5.1.1. Master–slave LCOs, equal-width coupling-pulse

The situation is explained in Fig. 10, showing the synchronization range, seen as a domain delimited by two thresholds beyond which the LCOs cannot synchronize any more, determined experimentally and numerically for a master–slave configuration. Except for the one-way setting, the equal-width coupling-pulse interaction is close to the usual coupling between mutually interacting LCOs, where coupling-pulses of similar width are the rule. Fig. 10(a) shows that the phase locking range contains only positive phase differences.

#### 5.1.2. Master (PG)–slave (LCO), narrow coupling-pulse

To analyze the coupling mechanism, we reduced the coupling flash (PG width pulse) to a quarter of its usual value. The positive phase differences involve a synchronization mechanism using the master’s narrow flash to shorten the integrating stage of the slave’s period. The negative phase differences show that phase locking may also be achieved by lengthening the firing stage of the slave’s period. Comparing Fig. 10(b) with the situation in Section 5.1.1, which shows only one polarity (phase differences positives), we deduce that the lengthening of the shorter part of the

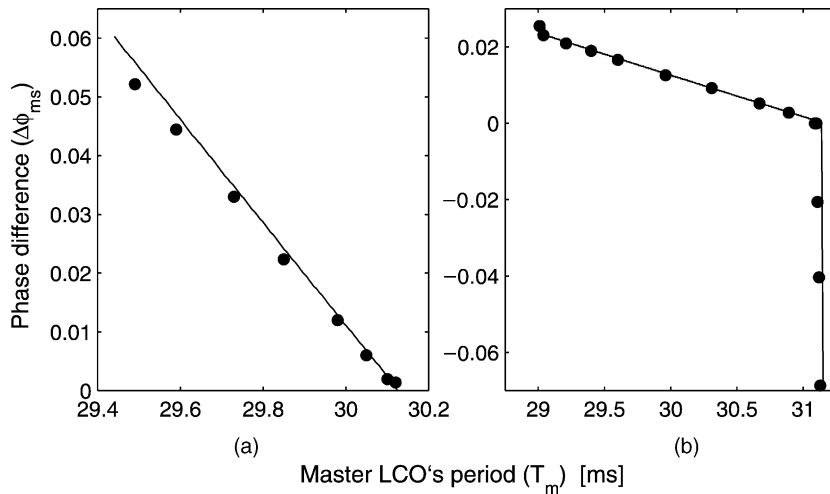


Fig. 10. Synchronization range in a master–slave situation. (a) Phase difference as a function of the master LCO's period. Experimental (●) and model (–) results are superimposed. The parameter values used for these measurements were:  $V_{Ms} = 8.95$  V,  $V_{Mm} = 8.96$  V,  $t_{ys} = 499.8$   $\mu$ s,  $t_{ym} = 500.4$   $\mu$ s,  $T_s = 30.11$  ms,  $\beta = 166.0$ ,  $d = 4.85$  cm. (b) Phase locking for a slave-LCO driven by a PG. The parameter values used were  $V_{Ms} = 8.99$  V,  $V_{Mm} = 9.04$  V,  $t_{ys} = 446$   $\mu$ s,  $t_{ym} = 112$   $\mu$ s,  $T_s = 31.12$  ms,  $\beta = 1270.9$  and  $d = 1.85$  cm.

period is of secondary importance in relation to the usual phase locking mechanism [33,34], which justifies the simplification used in Section 4.

### 5.1.3. Dual interaction setting

Both LCOs have the same mutual influence; they act on each other in the same way with equal strength, so they are interchangeable. The synchronization range (Fig. 11(a)) contains phase differences of both polarities, and the

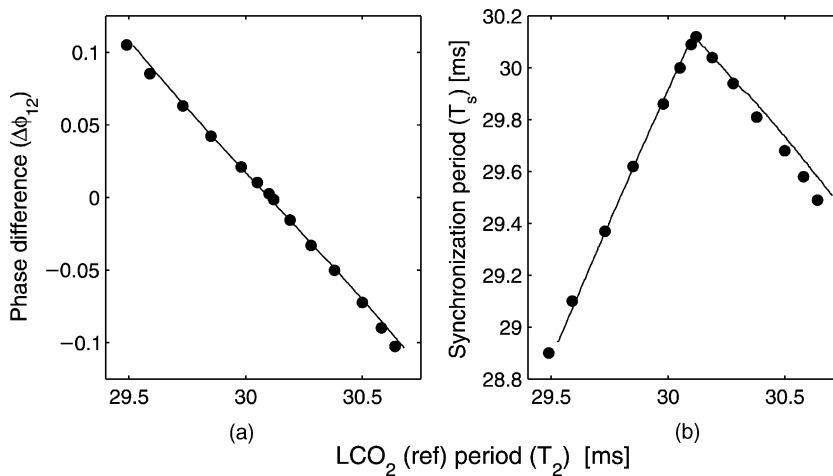


Fig. 11. Measurements of two LCOs with the same mutual influence. (a) Synchronization range. Experimental (●) and model (–) results of the synchronized phase differences as a function of the reference LCO's period. (b) Synchronization period as a function of the reference LCO's period. The experimental values for the parameters were  $V_{M1} = 8.95$  V,  $V_{M2} = 8.96$  V,  $t_{y1} = 499.8$   $\mu$ s,  $t_{y2} = 500.4$   $\mu$ s,  $T_1 = 30.11$  ms,  $\beta = 166.0$  and  $d = 4.85$  cm.

plot has an obvious symmetry confirming that the two LCOs are interchangeable. Fig. 11(b) shows that the period common to the two synchronized LCOs reaches a maximum value when the phase difference vanishes. Indeed, for zero phase difference, the coupling light pulses overlap, which results in lengthening of the firing stages and almost no shortening of the integrating stages. It is worthwhile to note that the synchronization range ( $\Delta T$ ) becomes larger when the strength  $\beta$  increases, the relationship between them being  $\Delta T \propto \beta \propto d^{-2}$ , where  $d$  denotes the distance between the light transmitter and the receptor of the interacting oscillators. For short distances (e.g. 2 cm) and large  $\beta$ , two LCOs with very different natural periods (up to 15% difference) are still able to synchronize.

Combining these considerations with results on synchronization time from Section 4, it is clear that the distance between LCOs plays an essential role in the establishment of phase locking. For distances near to the threshold, the synchronization time can be large. In this case, the system is not very robust, in the sense that if a perturbation acts on it, phase locking is broken and the system will take a lot of time to recover synchrony again.

It is interesting to note that a system composed of individuals with the same mutual influence shows a larger synchronization range than a master–slave system. This indicates that mutual interaction affords greater robustness to the system than a driven unidirectional interaction (master–slave).

In our experiments, we observed as expected only the synchronous state because the anti-synchronous state is, as we previously showed, unstable. Other experimental studies on coupled oscillators show the existence of multiple phase locked states [43,44] and in the case of identical oscillators, the coexistence of in-phase and anti-phase solutions. It is clear that our oscillators and the coupling involved are different to the Chua’s-like circuits used in [44] in the sense that the LCOs are relaxation oscillators and the interactions are pulsatile.

## 5.2. Three interacting LCOs in line

For sets of more than two LCOs, it is mandatory to specify the position of the reference LCO in the interacting ensemble. The measurements were obtained with a set of three LCOs in line:  $LCO_1 \leftrightarrow LCO_2 \leftrightarrow LCO_3$ , the only possible experimental configuration, the reference being  $LCO_2$ . The phase locking ranges were measured using two oscilloscopes triggered by the reference  $LCO_2$  [33]. There is an obvious symmetry in this case because the natural periods of  $LCO_1$  and  $LCO_3$  are similar. Fig. 12 shows that the phase differences can take either positive or negative values and  $\Delta\phi_{12}$  and  $\Delta\phi_{32}$  are always of opposite polarity, suggesting that  $LCO_1$  and  $LCO_3$  are indeed interchangeable. However, before synchronization has set in, it is not possible to foresee the mutually exclusive polarities, showing that a bifurcation-like phenomenon is present. Doing numerical integration, these states are dependent on the initial conditions. Experimental and theoretical results show that the synchronization range is similar in this situation compared to the case of two interacting LCOs. At the same time, numerical results show that the synchronization range can change with the configuration (for example, in the case of two, three, five and seven oscillators in line, the synchronization range  $\Delta T$  represents approximately 3% of the other LCOs’ period  $T$ ; for three equidistant oscillators in mutual interaction (ring configuration),  $\Delta T \approx 0.06T$ ; and for five oscillators arranged in a cross (i.e. there is one LCO that is able to interact mutually with the other ones and the other four LCOs are not able to interact with each other),  $\Delta T \approx 0.09T$ . For all cases, the distance considered is the same as that used in our experiment with three interacting LCOs in line.

Other experimental studies with three nearly identical oscillators deal principally with coupled oscillators in a ring configuration; e.g. in [45] (cited by Pikovsky et al. [13]) there are three stable synchronous configurations: in the first, all oscillators are synchronized in-phase, in the second, they are shifted in phase by  $2\pi/3$  with respect to the neighbor, and in the third, only two elements have the same phase. In [46,47], the system exhibits the in-phase and out-of-phase modes as well as multistability. In the coupled systems described above, the coupling is made via resistors or capacitors, in our case, the coupling is via light impulses. Another difference is that in our experiments, the coupling configuration is linear and not in a ring. Comparing our observations with the results in [45] (cited by

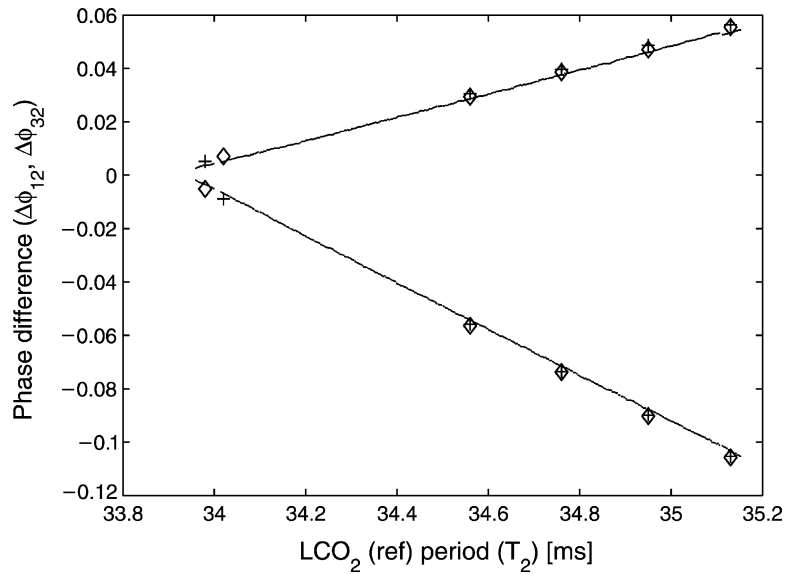


Fig. 12. Synchronization range for three interacting LCOs in line. Comparison between the experimental measurements ( $\diamond$  for  $\Delta\phi_{12}$ ,  $+$  for  $\Delta\phi_{32}$ ) and the mathematical model (—) for the phase locking region. The parameter values  $V_{M1} = 8.94$  V,  $V_{M2} = 8.99$  V,  $V_{M3} = 8.94$  V,  $t_{\gamma1} = 580.1$   $\mu$ s,  $t_{\gamma2} = 570.1$   $\mu$ s,  $t_{\gamma3} = 577.3$   $\mu$ s,  $T_1 = 33.98$  ms,  $T_3 = 33.99$  ms,  $\beta = 166.0$  and  $d = 4.85$  cm.

Pikovsky et al. [13]), we can say that when we approach the situation in which the three LCOs are nearly identical, we expect to obtain only one synchronous state with nearly zero phase difference. We suspect the existence of out-of-phase modes, but as in the case of two identical coupled LCOs, the range of initial conditions to achieve this state may be very narrow compared to the case of nearly in-phase synchronization. In [46,47], there is an analogy with our experiments, in the sense that one of the elements is detuned but the type of coupling is quite different, as well as the results.

## 6. Discussion and perspectives

The interest of the LCOs developed in this work lies in their simplicity. This allowed us to perform a detailed experimental study of how the LCOs synchronize [33], determine the synchronization range and the limits in which the system achieves a stable phase locking state, and finally develop a mathematical model based on the physical hardware which reproduces the experimental results.

This study of interacting LCOs has primarily been based on detailed observation of the individual phases as a function of the global parameters when the LCOs are coupled together to form a synchronized ensemble.

In this work, we have deliberately restricted our measurements, analysis and simulations to the study of phase locking between “similar” LCOs (1:1 synchronization), corresponding to firefly systems or potential technical applications (although it is evident that it could be extended to other synchronous regimes of arbitrary order  $n:m$  and analyze the transitions between quasi-periodicity and phase locking by means of Arnold tongues, in the plane frequency ( $\omega$ ), coupling strength ( $\beta$ )). The latter could be obtained by manually tuning the LCOs’ period.

Detailed quantitative observations of the phase locking between two LCOs emphasize the characteristics of the synchronization in an empirical way, giving the features that a theoretical model has to match. The model we present is based on the same physics that is involved in the LCO’s electronics; it is reliable and can be used to explore

situations that are not easily reproducible by experimental means. The mathematical analysis of the interaction of two identical LCOs shows that one has to consider two states: regular in-phase synchronization, showing the generalized tendency of the system to become synchronized, and an unstable state in which the system remains in anti-phase, rarely observed in the laboratory.

There is a nice analogy between LCOs and biological oscillators, and especially with social synchronization. Our results show that, despite intrinsic differences between LCOs, synchronization may be produced. This robustness is biologically important. Indeed, in a population, each individual has its own frequency, which is genetically or physiologically imposed. The simple interactions between the oscillators are enough, despite their differences, to produce synchronization. A consequence of this robustness would be the discovery of numerous natural systems governed by self-organized synchronization [16].

The results show that, the greater the symmetry of the interactions between oscillators, the easier and more robust the synchronization. Indeed, LCOs having the same rank (symmetrical interaction) are more robust (they tolerate higher intrinsic differences between their members to produce synchronization) than master–slave systems (asymmetrical interactions). The coupling depends on the distance between the LCOs and their configuration. There is a balance between inter-individual distances and the intrinsic differences between LCOs: the smaller the distance, the greater will be the difference between LCOs that is tolerated to produce synchronization.

Finally, as concluding remarks, we can point out that several technological systems could benefit from the concepts of synchronization and robustness. One of them involves collective robots, in which internal communication allows teammates to coordinate their movements and to generate spatial patterns. A classical problem is the synchronization of autonomous sensors distributed in the environment. This work is inspired by biological synchronization. One of the main questions in social biology is to understand the link between individual and collective behavior. Later results could lead us to propose a similar approach for the study of small groups of synchronized animals. Moreover, an elegant way to identify individual behavior would be the study of dynamics in a small mixed group of animals and robots [48] similar to LCOs and look at the response of the group when we change the behavior of the LCOs. The latter constitutes one of our research directions at present.

## Acknowledgements

We thank G. Nicolis and F. Moss for valuable discussions. We are grateful to D. Sanders and G. Ramsay for careful reading of the manuscript. The authors thank the anonymous referees for the helpful comments. GMRA acknowledges support from Belgian Technical Cooperation. JLD is research associate of the Belgian National Foundation for Scientific Research.

## References

- [1] H.G. Winful, L. Rahman, Synchronized chaos and spatiotemporal chaos in arrays of coupled lasers, *Phys. Rev. Lett.* 65 (1990) 1575–1578.
- [2] K. Wiesenfeld, P. Colet, S.H. Strogatz, Synchronization transitions in a disordered Josephson series array, *Phys. Rev. Lett.* 76 (1996) 404–407.
- [3] A. Hohl, A. Gavrielides, T. Erneux, V. Kovanis, Localized synchronization in two coupled nonidentical semiconductor lasers, *Phys. Rev. Lett.* 78 (1997) 4745–4748.
- [4] S.H. Strogatz, R.E. Mirollo, P.C. Matthews, Coupled nonlinear oscillators below the synchronization threshold: relaxation by generalized Landau damping, *Phys. Rev. Lett.* 68 (1992) 2730–2733.
- [5] I.Z. Kiss, Y. Zhai, J.L. Hudson, Collective dynamics of chaotic chemical oscillators and the law of large numbers, *Phys. Rev. Lett.* 88 (23) (2002) 238301.
- [6] A. Goldbeter, *Biochemical Oscillations and Cellular Rhythms—The Molecular Bases of Periodic and Chaotic Behaviour*, Cambridge University Press, Cambridge, 1996.

- [7] A.B. Neiman, D.F. Russell, X. Pei, W. Wojtenek, J. Twitty, E. Simonotto, B.A. Wettring, E. Wagner, L.A. Wilkens, F. Moss, Stochastic synchronization of electroreceptors in paddlefish, *Int. J. Bifurcat. Chaos* 10 (2000) 2499–2517.
- [8] V.S. Anishchenko, A.G. Balanov, N.B. Janson, N.B. Igosheva, G.V. Bordyugov, Entrainment between heart rate and weak noninvasive forcing, *Int. J. Bifurcat. Chaos* 10 (2000) 2339–2348.
- [9] C. Schäfer, M.G. Rosenblum, J. Kurths, H.H. Abel, Heartbeat synchronized with ventilation, *Nature* 392 (1998) 239–240.
- [10] C. Schäfer, M.G. Rosenblum, H.H. Abel, J. Kurths, Synchronization in the human cardiorespiratory system, *Phys. Rev. E* 60 (1999) 857–870.
- [11] B. Blasius, A. Huppert, L. Stone, Complex dynamics and phase synchronization in spatially extended ecological systems, *Nature* 399 (1999) 354–359.
- [12] B. Blasius, L. Stone, Chaos and phase synchronization in ecological systems, *Int. J. Bifurcat. Chaos* 10 (2000) 2361–2380.
- [13] A. Pikovsky, M. Rosenblum, J. Kurths, Synchronization—A Universal Concept in Nonlinear Sciences, Cambridge University Press, Cambridge, 2001.
- [14] I. Blekhan, Synchronization in Science and Technology, ASME, New York, 1988.
- [15] B.J. Cole, F.I. Trampus, Activity cycles in ant colonies; worker interactions and decentralized controls, in: C. Detrain, J.L. Deneubourg, J. Pasteels (Eds.), *Information Processing in Social Insects*, Birkhäuser, Basel, 1999.
- [16] S. Camazine, J.L. Deneubourg, S. Franks, J. Sneyd, G. Theraulaz, E. Bonabeau, *Self-organization in Biological Systems*, Princeton University Press, Princeton, NJ, 2001.
- [17] J. Buck, E. Buck, Synchronous fireflies, *Sci. Am.* 234 (1976) 74–85.
- [18] J. Buck, E. Buck, Toward a functional interpretation of synchronous flashing by fireflies, *Am. Nat.* 112 (1978) 471–492.
- [19] J.E. Lloyd, Fireflies of Melanesia: bioluminescence, mating behavior and synchronous flashing (Coleoptera: Lampyridae), *Environ. Entomol.* 2 (1973) 991–1008.
- [20] J.E. Lloyd, Model for the mating protocol of synchronously flashing fireflies, *Nature* 245 (1973) 268–270.
- [21] A. Moiseff, J. Copeland, A new type of synchronized flashing in a North America firefly, *J. Insect Behav.* 13 (2000) 597–612.
- [22] Y. Kuramoto, I. Nishikawa, Statistical macrodynamics of large dynamical systems. Case of a phase transition in oscillator communities, *J. Stat. Phys.* 49 (1987) 569–605.
- [23] J.J. Collins, I.N. Stewart, Coupled nonlinear oscillators and the symmetries of animal gaits, *J. Nonlin. Sci.* 3 (1993) 349–392.
- [24] U. Ernst, K. Pawelzik, T. Geisel, Delay-induced synchronization of biological oscillators, *Phys. Rev. E* 57 (1998) 2150–2162.
- [25] R.E. Mirollo, S.H. Strogatz, Synchronization of pulse-coupled biological oscillators, *SIAM J. Appl. Math.* 50 (1990) 1645–1662.
- [26] C.S. Peskin, *Mathematical Aspects of Heart Physiology*, Courant Institute of Mathematical Sciences, New York University, New York, 1975, pp. 268–278.
- [27] J. Jalife, Mutual entrainment and electrical coupling as mechanisms for synchronous firing of rabbit sino-atrial pace-maker cells, *J. Physiol.* 356 (1984) 221–243.
- [28] D.C. Michaels, E.P. Matyas, J. Jalife, Mechanisms of sinoatrial pacemaker synchronization: a new hypothesis, *Circ. Res.* 61 (1987) 704–714.
- [29] J. Buck, E. Buck, J.F. Case, F.E. Hanson, Control of flashing in fireflies. V. Pacemaker synchronization in *Pteroptyx cribellata*, *J. Comp. Physiol. A* 144 (1981) 287–298.
- [30] G.B. Ermentrout, An adaptive model for synchrony in the firefly *Pteroptyx malacca*, *J. Math. Biol.* 29 (1991) 571–585.
- [31] W. Garver, F. Moss, Electronic fireflies, *Sci. Am.* 269 (6) (1993) 128–130.
- [32] LINEAR Databook, LM555/LM555C Timer, National Semiconductor Corporation, no. 9, 1982, pp. 33–38.
- [33] J.L. Guisset, J.L. Deneubourg, G.M. Ramírez Ávila, The phase information associated to synchronized electronic fireflies, arXiv:nlin.AO/0206036, 2002.
- [34] J.L. Guisset, G.M. Ramírez Ávila, J.L. Deneubourg, Constructing coupled electronic fireflies and measuring their phase-locking behavior, *Rev. Bol. Fis.* 7 (2001) 102–114 (in Spanish).
- [35] C.H. Johnson, Phase response curves: what can they tell us about circadian clocks? in: T. Hiroshige, K. Honma (Eds.), *Circadian Clocks from Cell to Human*, Hokkaido University Press, Sapporo, 1992, pp. 209–249.
- [36] C.H. Johnson, Forty years of PRCs—what have we learned? *Chronobiol. Int.* 16 (6) (1999) 711–743.
- [37] B. Fuentes-Pardo, J. Ramos-Carvajal, The phase response curve of electroretinographic circadian rhythm of crayfish, *Comp. Biochem. Physiol. A* 74 (1983) 711–714.
- [38] A.T. Winfree, *The Geometry of Biological Time*, Springer, New York, 1980.
- [39] L. Glass, M. Mackey, *From Clocks to Chaos, The Rhythms of Life*, Princeton University Press, Princeton, NJ, 1988.
- [40] M. Nakao, K. Yamamoto, N. Katayama, M. Yamamoto, Phase shift of coupled oscillator model with feedbacks in response to multiple bright light exposure, *Psych. Clin. Neurosci.* 56 (3) (2002) 215–216.
- [41] P. Goel, B. Ermentrout, Synchrony, stability, and firing patterns in pulse-coupled oscillators, *Physica D* 163 (2002) 191–216.
- [42] M. Beckerman, *Adaptive Cooperative Systems*, Wiley, New York, NY, 1997.
- [43] A.A. Brailove, P.S. Linsay, An experimental study of a population of relaxation oscillators with a phase-repelling mean-field coupling, *Int. J. Bifurcat. Chaos* 6 (1996) 1211–1253.
- [44] D.V. Ramana Reddy, A. Sen, G.L. Johnston, Experimental evidence of time-delay-induced death in coupled limit cycle oscillators, *Phys. Rev. Lett.* 85 (2000) 3381–3384.
- [45] P.S. Landa, *Nonlinear Oscillations and Waves in Dynamical Systems*, Nauka, Moscow, 1980 (in Russian).

- [46] D. Ruwisch, M. Bode, D.V. Volkov, E.I. Volkov, Collective modes of three coupled relaxation oscillators: the influence of detuning, *Int. J. Bifurcat. Chaos* 9 (1999) 1969–1981.
- [47] E.I. Volkov, D.V. Volkov, Multirhythmicity generated by slow variable diffusion in a ring of relaxation oscillators and noise-induced abnormal interspike variability, *Phys. Rev. E* 65 (2002) 046232.
- [48] G. De Schutter, G. Theraulaz, J.L. Deneubourg, Animal-robots collective intelligence, *Ann. Math. Art. Int.* 31 (2001) 223–238.